Eur. Phys. J. C (2013) 73:2581
DOI 10.1140/epjc/s10052-013-2581-9

THE EUROPEAN PHYSICAL JOURNAL C

Regular Article - Experimental Physics

Study of $\Sigma(1385)$ and $\Xi(1321)$ hyperon and antihyperon production in deep inelastic muon scattering

C. Adolph[8], M.G. Alekseev[24], V.Y. Alexakhin[7], Y. Alexandrov[15,b], G.D. Alexeev[7], A. Amoroso[27], A. Austregesilo[10,17], B. Badełek[31], F. Balestra[27], J. Barth[4], G. Baum[1], Y. Bedfer[22], A. Berlin[2], J. Bernhard[13], R. Bertini[27], K. Bicker[10,17], J. Bieling[4], R. Birsa[24], J. Bisplinghoff[3], P. Bordalo[12,c], F. Bradamante[25], C. Braun[8], A. Bravar[24], A. Bressan[25,a], M. Büchele[9], E. Burtin[22], L. Capozza[22], M. Chiosso[27], S.U. Chung[17,d], A. Cicuttin[26], M.L. Crespo[26], S. Dalla Torre[24], S.S. Dasgupta[24], S. Dasgupta[6], O.Y. Denisov[28], S.V. Donskov[21], N. Doshita[33], V. Duic[25], W. Dünnweber[16], M. Dziewiecki[32], A. Efremov[7], C. Elia[25], P.D. Eversheim[3], W. Eyrich[8], M. Faessler[16], A. Ferrero[22], A. Filin[21], M. Finger[19], M. Finger Jr.[19], H. Fischer[9], C. Franco[12], N. du Fresne von Hohenesche[13,10], J.M. Friedrich[17], V. Frolov[10], R. Garfagnini[27], F. Gautheron[2], O.P. Gavrichtchouk[7], S. Gerassimov[15,17], R. Geyer[16], M. Giorgi[25], I. Gnesi[27], B. Gobbo[24], S. Goertz[4], S. Grabmüller[17], A. Grasso[27], B. Grube[17], R. Gushterski[7], A. Guskov[7], T. Guthörl[9,e], F. Haas[17], D. von Harrach[13], F.H. Heinsius[9], F. Herrmann[9], C. Heß[2], F. Hinterberger[3], C. Höppner[17], N. Horikawa[18,f], N. d'Hose[22], S. Huber[17], S. Ishimoto[33,g], Y. Ivanshin[7], T. Iwata[33], R. Jahn[3], V. Jary[20], P. Jasinski[13], R. Joosten[3], E. Kabuß[13], D. Kang[13], B. Ketzer[17], G.V. Khaustov[21], Y.A. Khokhlov[21,h], Y. Kisselev[2], F. Klein[4], K. Klimaszewski[30], J.H. Koivuniemi[2], V.N. Kolosov[21], K. Kondo[33], K. Königsmann[9], I. Konorov[15,17], V.F. Konstantinov[21], A.M. Kotzinian[27], O. Kouznetsov[7,22], M. Krämer[17], Z.V. Kroumchtein[7], N. Kuchinski[7], F. Kunne[22], K. Kurek[30], R.P. Kurjata[32], A.A. Lednev[21], A. Lehmann[8], S. Levorato[25], J. Lichtenstadt[23], A. Maggiora[28], A. Magnon[22], N. Makke[22,25], G.K. Mallot[10], A. Mann[17], C. Marchand[22], A. Martin[25], J. Marzec[32], H. Matsuda[33], T. Matsuda[14], G. Meshcheryakov[7], W. Meyer[2], T. Michigami[33], Y.V. Mikhailov[21], Y. Miyachi[33], A. Morreale[22,i], A. Nagaytsev[7], T. Nagel[17], F. Nerling[9], S. Neubert[17], D. Neyret[22], V.I. Nikolaenko[21], J. Novy[19], W.-D. Nowak[9], A.S. Nunes[12], A.G. Olshevsky[7], M. Ostrick[13], R. Panknin[4], D. Panzieri[29], B. Parsamyan[27], S. Paul[17], G. Piragino[27], S. Platchkov[22], J. Pochodzalla[13], J. Polak[11,25], V.A. Polyakov[21], J. Pretz[4,j], M. Quaresma[12], C. Quintans[12], S. Ramos[12,c], G. Reicherz[2], E. Rocco[10], V. Rodionov[7], E. Rondio[30], N.S. Rossiyskaya[7], D.I. Ryabchikov[21], V.D. Samoylenko[21], A. Sandacz[30], M.G. Sapozhnikov[7], S. Sarkar[6], I.A. Savin[7], G. Sbrizzai[25], P. Schiavon[25], C. Schill[9], T. Schlüter[16], A. Schmidt[8], K. Schmidt[9,e], L. Schmitt[17,k], H. Schmïden[3], K. Schönning[10], S. Schopferer[9], M. Schott[10], O.Y. Shevchenko[7], L. Silva[12], L. Sinha[6], S. Sirtl[9], S. Sosio[27], F. Sozzi[24], A. Srnka[5], L. Steiger[24], M. Stolarski[12], M. Sulc[11], R. Sulej[30], H. Suzuki[33,f], P. Sznajder[30], S. Takekawa[28], J. Ter Wolbeek[9,e], S. Tessaro[24], F. Tessarotto[24], F. Thibaud[22], S. Uhl[17], I. Uman[16], M. Vandenbroucke[22], M. Virius[20], L. Wang[2], T. Weisrock[13], M. Wilfert[13], R. Windmolders[4], W. Wiślicki[30], H. Wollny[22], K. Zaremba[32], M. Zavertyaev[15], E. Zemlyanichkina[7], N. Zhuravlev[7], M. Ziembicki[32]

[1] Fakultät für Physik, Universität Bielefeld, 33501 Bielefeld, Germany[l]
[2] Institut für Experimentalphysik, Universität Bochum, 44780 Bochum, Germany[l]
[3] Helmholtz-Institut für Strahlen- und Kernphysik, Universität Bonn, 53115 Bonn, Germany[l]
[4] Physikalisches Institut, Universität Bonn, 53115 Bonn, Germany[l]
[5] Institute of Scientific Instruments, AS CR, 61264 Brno, Czech Republic[m]
[6] Matrivani Institute of Experimental Research & Education, Calcutta 700 030, India[n]
[7] Joint Institute for Nuclear Research, 141980 Dubna, Moscow region, Russia[o]
[8] Physikalisches Institut, Universität Erlangen–Nürnberg, 91054 Erlangen, Germany[l]
[9] Physikalisches Institut, Universität Freiburg, 79104 Freiburg, Germany[l,s]
[10] CERN, 1211 Geneva 23, Switzerland
[11] Technical University in Liberec, 46117 Liberec, Czech Republic[m]
[12] LIP, 1000-149 Lisbon, Portugal[p]
[13] Institut für Kernphysik, Universität Mainz, 55099 Mainz, Germany[l]
[14] University of Miyazaki, Miyazaki 889-2192, Japan[q]
[15] Lebedev Physical Institute, 119991 Moscow, Russia
[16] Department für Physik, Ludwig-Maximilians-Universität München, 80799 Munich, Germany[l,r]
[17] Technische Universität München, Physik Department, 85748 Garching, Germany[l,r]
[18] Nagoya University, 464 Nagoya, Japan[q]
[19] Faculty of Mathematics and Physics, Charles University in Prague, 18000 Prague, Czech Republic[m]
[20] Czech Technical University in Prague, 16636 Prague, Czech Republic[m,s]

[21] Institute for High Energy Physics, State Research Center of the Russian Federation, 142281 Protvino, Russia
[22] CEA IRFU/SPhN Saclay, 91191 Gif-sur-Yvette, France[s]
[23] School of Physics and Astronomy, Tel Aviv University, 69978 Tel Aviv, Israel[t]
[24] Trieste Section of INFN, 34127 Trieste, Italy
[25] Department of Physics and Trieste Section of INFN, University of Trieste, 34127 Trieste, Italy
[26] Abdus Salam ICTP and Trieste Section of INFN, 34127 Trieste, Italy
[27] Department of Physics and Torino Section of INFN, University of Turin, 10125 Turin, Italy
[28] Torino Section of INFN, 10125 Turin, Italy
[29] University of Eastern Piedmont, 15100 Alessandria, Italy
[30] National Centre for Nuclear Research, 00-681 Warsaw, Poland[u]
[31] Faculty of Physics, University of Warsaw, 00-681 Warsaw, Poland[u]
[32] Institute of Radioelectronics, Warsaw University of Technology, 00-665 Warsaw, Poland[u]
[33] Yamagata University, Yamagata 992-8510, Japan[q]

Received: 3 April 2013 / Revised: 21 August 2013 / Published online: 9 October 2013

Abstract Large samples of Λ, $\Sigma(1385)$ and $\Xi(1321)$ hyperons produced in the deep-inelastic muon scattering off a ^{6}LiD target were collected with the COMPASS experimental setup at CERN. The relative yields of $\Sigma(1385)^+$, $\Sigma(1385)^-$, $\bar{\Sigma}(1385)^-$, $\bar{\Sigma}(1385)^+$, $\Xi(1321)^-$, and $\bar{\Xi}(1321)^+$ hyperons decaying into $\Lambda(\bar{\Lambda})\pi$ were measured. The ratios of heavy-hyperon to Λ and heavy-antihyperon to $\bar{\Lambda}$ were found to be in the range 3.8 % to 5.6 % with a relative uncertainty of about 10 %. They were used to tune the parameters relevant for strange particle production of the LEPTO Monte Carlo generator.

1 Introduction

The study of hyperon production in deep inelastic scattering (DIS) is important for a better understanding of the role of strange quarks in the nucleon structure and in the hadronization process. The lightest hyperon, the Λ baryon, was studied in most detail. In addition to Λ from direct production, a significant fraction of Λ particles originates from the decay of heavier hyperons such as Σ^0, Σ^*, or Ξ. The notation for $\Sigma(1385)$ and $\Xi(1321)$ will be used without indicating mass values, and with the "*" symbol for $\Sigma(1385)$ in order to distinguish the $J^P = 3/2^+$ Σ hyperons from the $J^P = 1/2^+$ ones. An indirect Λ production from hyperons decays is also included in the measurements of the longitudinal spin transfer to the Λ hyperon in polarised DIS [1, 2]. Using a Monte Carlo simulation based on the Lund string fragmentation model [3], the authors of Ref. [1] have estimated that only about 40 % of the produced Λ baryons originate from direct string fragmentation.

The production of Σ^0, Σ^{*+}, Σ^{*-} and Ξ^- hyperons with neutrino beams was reported by the NOMAD Collaboration [4]. Information on the production of these heavy hyperons with muon or electron beams is still missing. To our knowledge, the production of the antiparticles, $\bar{\Sigma}^{*-}$, $\bar{\Sigma}^{*+}$, and $\bar{\Xi}$ has never been studied in DIS. New data are hence required in order to produce reliable numerical estimate of heavy hyperon production rates in DIS.

[a] e-mail: Andrea.Bressan@cern.ch

[b] Deceased.

[c] Also at IST, Universidade Técnica de Lisboa, Lisbon, Portugal.

[d] Also at Department of Physics, Pusan National University, Busan 609-735, Republic of Korea and at Physics Department, Brookhaven National Laboratory, Upton, NY 11973, USA.

[e] Supported by the DFG Research Training Group Programme 1102 "Physics at Hadron Accelerators".

[f] Also at Chubu University, Kasugai, Aichi 487-8501, Japan.

[g] Also at KEK, 1-1 Oho, Tsukuba, Ibaraki 305-0801, Japan.

[h] Also at Moscow Institute of Physics and Technology, Moscow Region 141700, Russia.

[i] Present address: National Science Foundation, 4201 Wilson Boulevard, Arlington, VA 22230, USA.

[j] Present address: RWTH Aachen University, III. Physikalisches Institut, 52056 Aachen, Germany.

[k] Also at GSI mbH, Planckstr. 1, 64291 Darmstadt, Germany.

[l] Supported by the German Bundesministerium für Bildung und Forschung.

[m] Supported by Czech Republic MEYS Grants ME492 and LA242.

[n] Supported by SAIL (CSR), Govt. of India.

[o] Supported by CERN-RFBR Grants 08-02-91009 and 12-02-91500.

[p] Supported by the Portuguese FCT—Fundação para a Ciência e Tecnologia, COMPETE and QREN, Grants CERN/FP/109323/2009, CERN/FP/116376/2010 and CERN/FP/123600/2011.

[q] Supported by the MEXT and the JSPS under the Grants No. 18002006, No. 20540299 and No. 18540281; Daiko Foundation and Yamada Foundation

[r] Supported by the DFG cluster of excellence 'Origin and Structure of the Universe' (www.universe-cluster.de)

[s] Supported by EU FP7 (HadronPhysics3, Grant Agreement number 283286)

[t] Supported by the Israel Science Foundation, founded by the Israel Academy of Sciences and Humanities

[u] Supported by the Polish NCN Grant DEC-2011/01/M/ST2/02350

In this Paper, the production rates of Σ^{*+}, Σ^{*-}, Ξ and their antiparticles are presented and compared to those of Λ and $\bar{\Lambda}$ hyperons. The resulting values are used to constrain the parameters of the JETSET package whith is embedded in the LEPTO Monte Carlo generator.

2 The experimental setup

The data used in the present analysis were collected by the COMPASS Collaboration at CERN during the years 2003–2004. The experiment was performed at the CERN M2 muon beam line. The μ^+ beam intensity was 2×10^8 per spill of 4.8 s, with a cycle time of 16.8 s. The average beam momentum was 160 GeV/c. The μ^+ beam is naturally polarised by the weak decays of the parent hadrons.

The beam traverses two cylindrical cells of a polarised ^{6}LiD target, both of 60 cm length and 3 cm diameter. The target material in the neighbouring cells is polarised longitudinally in opposite directions with respect to the beam. However, the target polarisation values are not used in this study. The data from both target cells and polarisations are combined.

The COMPASS experimental setup was designed to detect both scattered muons and produced hadrons in wide momentum and angular ranges. It consists of two spectrometer stages, each comprising a large-aperture dipole magnet. The aperture of the target magnet limits the acceptance to ± 70 mrad at the upstream end of the target. Muons are identified in large area tracking detectors and scintillators downstream of concrete or iron muon filters. Hadrons are detected in two hadron calorimeters installed upstream of the muon filters.

Data recording is activated by inclusive and semi-inclusive triggers indicating the presence of a scattered muon and emitted hadrons, respectively. The trigger system covers a wide range of Q^2 from quasi-real photoproduction to deep inelastic interactions. A more detailed description of the COMPASS apparatus can be found in Ref. [5].

3 Λ and $\bar{\Lambda}$ hyperon samples

The event selection requires a reconstructed interaction vertex that is defined by the incoming and the scattered muon and located within the target. DIS events are selected by cuts on the four-momentum squared of the virtual photon, $Q^2 > 1$ (GeV/c)^2, and on the fractional energy y of the virtual photon, $0.2 < y < 0.9$. The latter cut removes events with large radiative corrections at large y and with poorly reconstructed kinematic variables at low y. The resulting data sample consists of 3.12×10^8 events. The Λ and $\bar{\Lambda}$ hyperons are identified by their decays into $p\pi^-$ and $\bar{p}\pi^+$,

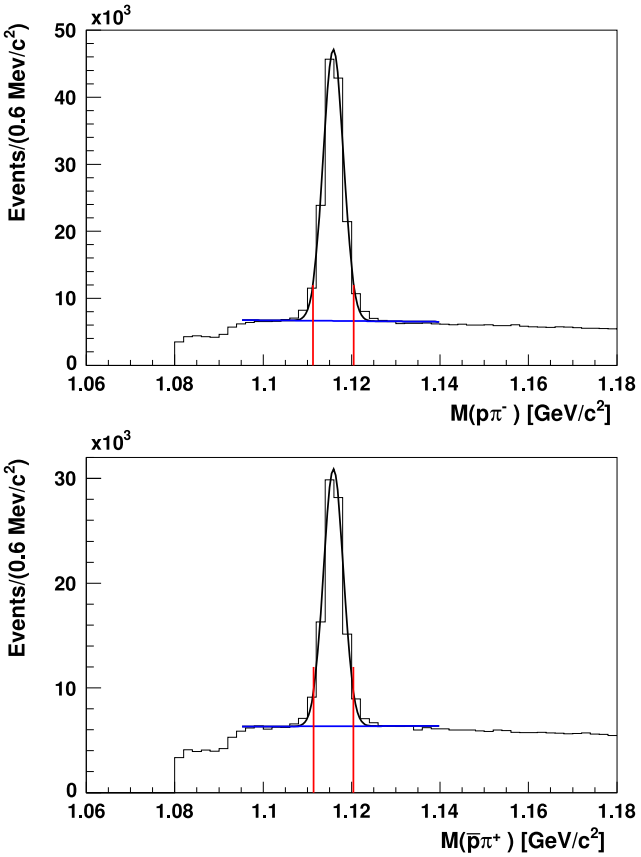

Fig. 1 The $p\pi^-$ (*top*) and $\bar{p}\pi^+$ (*bottom*) invariant mass distributions. The total numbers of Λ and $\bar{\Lambda}$ determined within the fit interval (see text) are $N(\Lambda) = 112449 \pm 418$ and $N(\bar{\Lambda}) = 66685 \pm 350$. The *vertical lines* mark the $\pm 2\sigma$ intervals of the $\Lambda(\bar{\Lambda})$ signals used for the Σ^*, Ξ and their antiparticle search

respectively. In order to evaluate possible systematic effects, decays of K^0_s into $\pi^-\pi^+$ were also analysed. The K^0_s background was already disscused in details in Ref. [2]. Candidate events for Λ, $\bar{\Lambda}$ and K^0_s were selected by requiring that two hadron tracks form a secondary vertex located within a 105 cm long fiducial region starting 5 cm downstream of the target. Outside this region, decay-hadron tracks cannot be reconstructed with sufficient resolution. Vertices with identified muons or electrons were removed. Only hadrons with momenta larger than 1 GeV/c were retained, guaranteeing a good reconstruction efficiency. A further cut was imposed on the transverse momentum p_T of the decay products with respect to the hyperon direction, $p_T > 23$ MeV/c, in order to reject e^+e^- pairs from γ-conversion. Using the Feynman variable x_F, the $\Lambda(\bar{\Lambda})$ candidates were selected in the current fragmentation region requiring $x_F > 0.05$.

The invariant mass distributions for two-hadron events, which are assumed to be either $p\pi^-$ or $\bar{p}\pi^+$ pairs, are shown in Fig. 1. The distributions were fitted in the interval 1.095–1.140 GeV/c^2 with a sum of a Gaussian function for the signal and a third-order polynomial for the background.

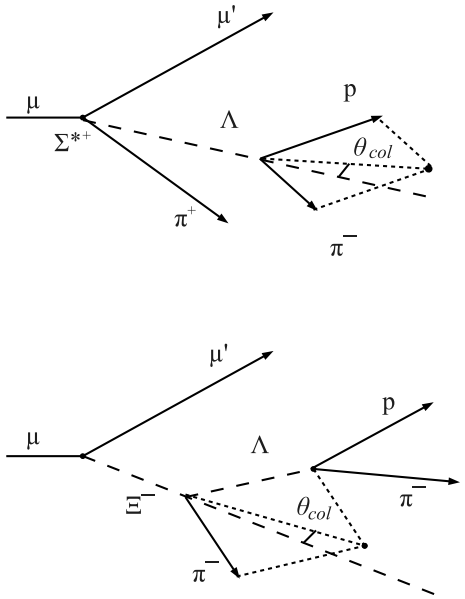

Fig. 2 Schematic picture of the Σ^{*+} strong decay (*top*) and of the Ξ^- weak decay (*bottom*)

The total numbers of Λ and $\bar{\Lambda}$ hyperons, represents an improvement of an order of magnitude[1] with respect to previous experiments [1, 6–9]. The invariant mass resolutions for Λ and $\bar{\Lambda}$ are 2.22 ± 0.01 MeV/c^2 and 2.21 ± 0.01 MeV/c^2, respectively.

The Λ hyperons in the resulting event samples are either directly produced or originate from the decay of heavier hyperons. The Σ^* and Ξ hyperons and their antiparticle partners decay with fractions of 87.5 % or 99.9 %, respectively, into $\Lambda(\bar{\Lambda})\pi^{\pm}$. The production and the decay of the Σ^* hyperon is illustrated in Fig. 2 (top). Since the Σ^* decays via strong interaction, the production and decay vertices are indistinguishable. The secondary vertex is the signature of the $\Lambda(\bar{\Lambda})$ weak decay. In contrast, the Ξ hyperon decays via weak interaction (Fig. 2 (bottom)), such that the decay vertex is clearly separated from the production vertex.

4 Σ^* and Ξ hyperon samples

The search for Σ^* hyperons was performed using the samples obtained after a collinearity cut. This cut requires that the angle $\theta_{\rm col}$ between the Λ momentum and the line connecting the primary and the secondary vertex is smaller than 0.01 rad. It ensures predominant selection of Λ baryons pointing to the primary vertex and removes only 10 % of their total yield. The $p\pi^-(\bar{p}\pi^+)$ pairs within a $\pm 2\sigma$ mass interval from the mean value of the $\Lambda(\bar{\Lambda})$ peak were then combined with a charged track from the primary vertex, which is assumed to be a pion. All possible combinations were taken into account. The resulting $\Lambda\pi$ invariant mass distributions are shown in Fig. 3. The peaks for Σ^{*+}, $\bar{\Sigma}^{*-}$, Σ^{*-}, and $\bar{\Sigma}^{*+}$ production are clearly visible. In the two bottom panels, the small additional peaks of Ξ^- and $\bar{\Xi}^+$ are also visible, despite the fact that the $\Lambda(\bar{\Lambda})$ from the decays of these hyperons originate not from the primary vertex. The 1σ mass resolutions for Σ^* and $\bar{\Sigma}^*$ agree within uncertainties: 9.3 ± 3.6 MeV/c^2 for Σ^{*+}, 6.1 ± 2.7 MeV/c^2 for $\bar{\Sigma}^{*-}$, 8.7 ± 3.5 MeV/c^2 for Σ^{*-} and 7.1 ± 2.1 MeV/c^2 for $\bar{\Sigma}^{*+}$.

An alternative method was chosen to search for Ξ hyperons, for which the primary and the secondary decay vertices are clearly separated (Fig. 2 (bottom)). The Ξ hyperons were identified using a two dimensional Closest Distance of Approach (CDA) procedure. The CDA values were calculated between the $\Lambda(\bar{\Lambda})$ line of flight and a charged particle track not associated to the primary vertex. The Λ baryons were taken from the samples shown in Fig. 1. A collinearity cut was then imposed on the direction of the Ξ momentum and the line connecting it to the primary vertex. The value of the cut, $\theta_{\rm col} < 0.02$ rad, is larger than the value used for Σ^* reconstruction, since the direction of the Ξ is reconstructed less precisely than that for Λ. The invariant mass distributions are shown in Fig. 4. The resulting resolutions for Ξ and $\bar{\Xi}$ are the same: 2.8 ± 0.1 MeV/c^2.

In order to extract the yield ratios of heavy hyperons to Λ baryons, the ratios of the corresponding acceptances had to be evaluated. It should be noted that the acceptance corrections were evaluated only for the region $Q^2 > 1$ (GeV/c)^2. The calculation was done using a Monte Carlo simulation based on the LEPTO 6.5.1 generator for DIS events with default parameters, and a full spectrometer description based on GEANT 3.21. For each hyperon, the acceptance was calculated as the ratio of $N_{\rm rec}$, the number of reconstructed hyperons, and $N_{\rm gen}$, the number of hyperons generated by LEPTO. The same reconstruction and selection procedure were used as for the real data.

The resulting values of the acceptance ratios for Σ^* to Λ and for Ξ to Λ are 0.67 and 0.42, respectively. The difference between Σ^* and Ξ acceptance ratios is explained by different decay patterns: the Σ^* hyperons decay practically at the primary vertex, while for the Ξ hyperons there exists a secondary one. The acceptance ratio also includes a correction for the branching ratio, $\mathrm{Br}(\Sigma^* \to \Lambda\pi) = 0.88 \pm 0.02$ [10]. It should be noted that Figs. 1, 3, 4 are not acceptance-corrected.

The invariant mass distributions for Σ^{*+} and $\bar{\Sigma}^{*-}$ (Fig. 3 (top)) were fitted by a sum of a signal function, $S(x)$, described by a convolution of a Breit-Wigner and a Gaussian, and a background function $B(x)$:

$$S(x) = \frac{\Gamma}{(2\pi)^{3/2}} \int \frac{N e^{-\frac{1}{2}(\frac{t-x}{\sigma})^2}}{(t-M)^2 + (\frac{\Gamma}{2})^2}\, dt; \qquad (1)$$

[1] The samples used in the Λ analysis [2] and in this Paper are different due to different cuts.

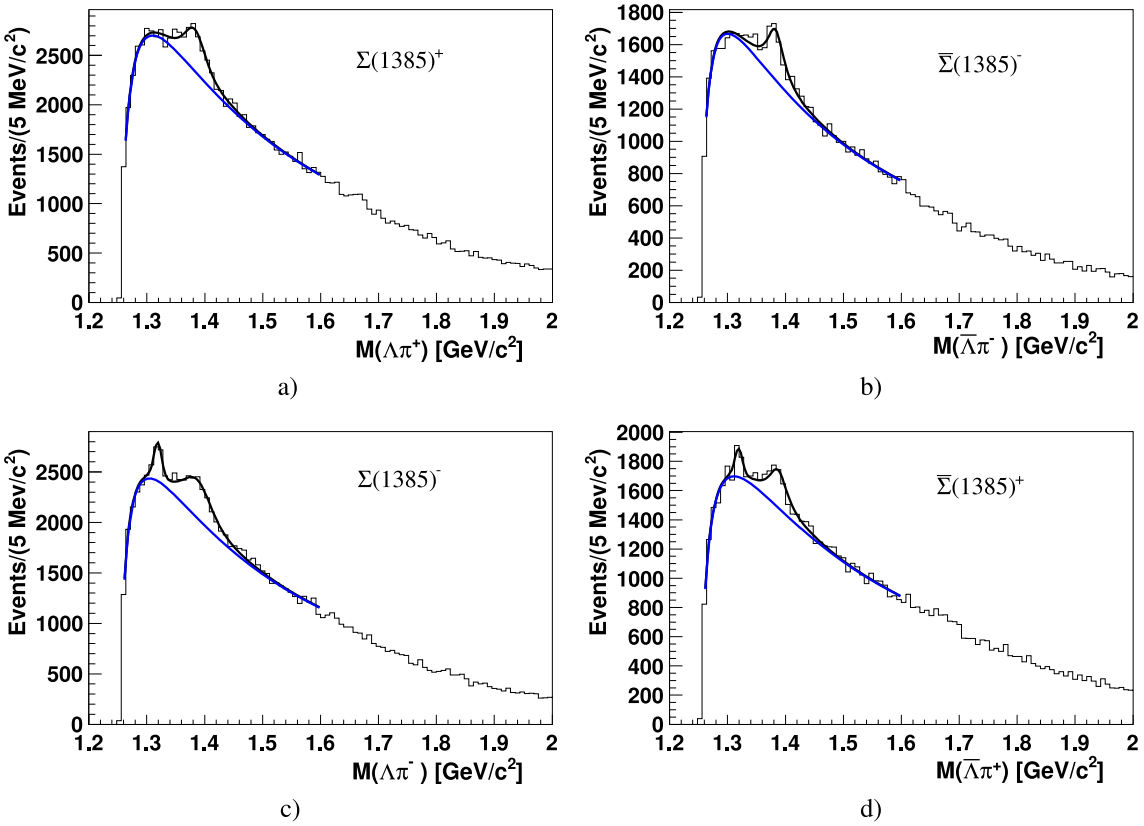

Fig. 3 The $\Lambda\pi$ invariant mass distributions. The *solid lines* represent the signal plus backgroud and the background only obtained from the fit. The signals include peaks for the following candidates: (**a**) $\Sigma^{*+} \to \Lambda\pi^+$; (**b**) $\bar{\Sigma}^{*-} \to \bar{\Lambda}\pi^-$; (**c**) $\Sigma^{*-} \to \Lambda\pi^-$ and $\Xi^- \to \Lambda\pi^-$; (**d**) $\bar{\Sigma}^{*+} \to \bar{\Lambda}\pi^+$ and $\bar{\Xi}^+ \to \bar{\Lambda}\pi^+$. The number of Σ^* resulting from the fits are: $N(\Sigma^{*+}) = 3631 \pm 333$, $N(\Sigma^{*-}) = 2970 \pm 490$, $N(\bar{\Sigma}^{*-}) = 2173 \pm 222$ and $N(\bar{\Sigma}^{*+}) = 1889 \pm 265$

$$B(x) = a(x - M_{\text{th}})^b e^{-c(x-M_{\text{th}})^d}. \quad (2)$$

The two other invariant mass distributions, $\Lambda\pi^-$ and $\bar{\Lambda}\pi^+$, include contributions coming from the Ξ decay (Fig. 3 (bottom)). These contributions were taken into account by adding a second Gaussian function to the signal. The values of hyperon mass M and width Γ were fixed to the PDG values [10]. The value of $M_{\text{th}} = 1254$ MeV was chosen to be the sum of Λ and π masses, and a, b, c and d were free parameters.

The invariant mass distributions shown for Ξ^- and $\bar{\Xi}^+$ in Fig. 4 were fitted by a sum of a Gaussian function for the signal and a function $B(x)$ for the background, described by an analogous parameterisation as the one used for Σ^*, given in Eq. (2). It should be noted that a first study of Ξ production using COMPASS data was done for the pentaquark $\Phi(1860)$ search [11].

5 Discussion of results

The ratios of the acceptance-corrected yields of Σ^* and Ξ to that of Λ hyperons are given in Table 1 along with their statistical and systematic uncertainties. Three sources of systematic uncertainties were considered:

(a) The uncertainty on the number of hyperon events was estimated by varying the width of the window for the selection of Λ and $\bar{\Lambda}$ samples, from $\pm 2\sigma$ to $\pm 2.5\sigma$ and to $\pm 1.5\sigma$. This variation results in differences of 0.003, 0.002, 0.002, and 0.002 for the relative yields of Σ^{*+}, $\bar{\Sigma}^{*-}$, Σ^{*-}, and $\bar{\Sigma}^{*+}$, respectively. The corresponding values for the relative yields of Ξ^- and $\bar{\Xi}^+$ are equal to 0.001.

(b) The systematic uncertainties coming from the evaluation of the background were estimated using a mixed event method. In this method, the shape of the background in the $\Lambda\pi$ invariant-mass distribution was determined by combining lambdas and pions from different events. The energies of these pions were chosen to be similar to the energy of the pion from the Λ decay. The standard collinearity cut (θ_{col}) was also applied. The uncertainties resulting from this procedure are 0.003, 0.004, 0.004, and 0.005 for the relative yields of Σ^{*+}, $\bar{\Sigma}^{*-}$, Σ^{*-}, and $\bar{\Sigma}^{*+}$, respectively. The uncertainties for

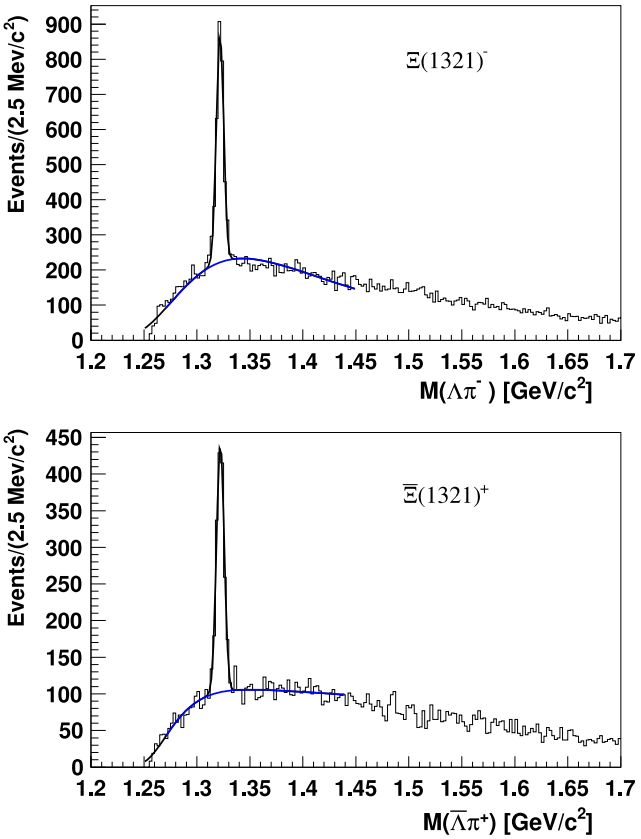

Fig. 4 Invariant mass distributions for $\Lambda\pi^-$ (*top*) and $\bar{\Lambda}\pi^+$ (*bottom*) pairs. The *solid lines* represent the signal plus backgroud and the background only obtained from the fit. The peaks correspond to $\Xi^- \to \Lambda\pi^-$ (*top*) and $\bar{\Xi}^+ \to \bar{\Lambda}\pi^+$ (*bottom*) candidates. The estimated numbers of Ξ hyperons are: $N(\Xi^-) = 2320 \pm 68$ and $N(\bar{\Xi}^+) = 1147 \pm 49$

the relative yields of Ξ^- and $\bar{\Xi}^+$ were found to be negligible.

(c) The systematic uncertainties on the acceptance arising from tuning the Monte Carlo parameters were evaluated to be 0.003, 0.004, 0.005, and 0.003 for Σ^{*+}, $\bar{\Sigma}^{*-}$, Σ^{*-}, and $\bar{\Sigma}^{*+}$, respectively. For Ξ^- and $\bar{\Xi}^+$ these uncertainties are 0.002.

The combined systematic uncertainties were calculated by summing quadratically these three contributions.

The experimental ratios show that the number of heavier hyperons compared to that of Λ hyperons is small, in the range 3.8 % to 5.6 %. The results also indicate that the percentage of Λ originating from the decay of Σ^* and Ξ hyperons is almost the same (within quoted uncertainties) as the percentage of $\bar{\Lambda}$ originating from the decay of the respective antiparticles.

The ratios of production yields of hyperons and antihyperons to those of Λ and $\bar{\Lambda}$ are obtained for the first time in charged lepton DIS reactions. Earlier, only hyperon to Λ yields, but no yields for antiparticles, were measured in neutrino DIS by the NOMAD Collaboration [4]. The NOMAD values are also shown in Table 1; the average neutrino energy of charged current interactions was 45.3 GeV. We note that COMPASS has collected considerably larger (from 30 to 130 times) samples of hyperons than NOMAD in the current fragmentation region. It is interesting to compare the charged lepton and the neutrino data despite the different underlying interactions. COMPASS measures similar values for the Σ^{*+}/Λ and Σ^{*-}/Λ ratios. Taking into account experimental uncertainties, the same conclusion is valid for NOMAD data but with NOMAD values being a factor of two smaller than the COMPASS ones. Finally, within uncertainties, the Ξ^-/Λ yield ratio measured by NOMAD is consistent with zero, while COMPASS gives comparable and non-zero values for Ξ^-/Λ and $\bar{\Xi}^+/\bar{\Lambda}$ ratios. The large experimental uncertainties in the NOMAD measurements prevent us from drawing conclusions about heavy hyperon production in charged lepton DIS as compared to neutrino DIS.

Table 1 The heavy hyperon to Λ and antihyperon to $\bar{\Lambda}$ yield ratios in lepton DIS. The results are compared with those from NOMAD [4] neutrino DIS data in the current fragmentation region.[3] The average neutrino energy of charged current interactions was 45.3 GeV

Ratios	This work	NOMAD
Σ^{*+}/Λ	$0.055 \pm 0.005(\text{stat}) \pm 0.005(\text{syst})$	0.025 ± 0.019
$\bar{\Sigma}^{*-}/\bar{\Lambda}$	$0.047 \pm 0.006(\text{stat}) \pm 0.006(\text{syst})$	–
Σ^{*-}/Λ	$0.056 \pm 0.009(\text{stat}) \pm 0.007(\text{syst})$	0.037 ± 0.015
$\bar{\Sigma}^{*+}/\bar{\Lambda}$	$0.039 \pm 0.006(\text{stat}) \pm 0.006(\text{syst})$	–
Ξ^-/Λ	$0.038 \pm 0.003(\text{stat}) \pm 0.002(\text{syst})$	0.007 ± 0.007
$\bar{\Xi}^+/\bar{\Lambda}$	$0.043 \pm 0.004(\text{stat}) \pm 0.002(\text{syst})$	–

In a different approach, the same COMPASS yield ratios as discussed above were also evaluated after removing the DIS cuts $Q^2 > 1$ (GeV/c)^2 and $0.2 < y < 0.9$. Only the initial selection for $\Lambda(\bar{\Lambda})$ candidates was applied: (a) events with two oppositely charged hadron tracks form the secondary vertex, (b) hadrons with momenta larger than 1 GeV/c, (c) $p_T > 23$ MeV/c on the transverse momentum of the decay products with respect to the hyperon direction, (d) $\Lambda(\bar{\Lambda})$ candidates in the current fragmentation region $x_F > 0.05$.

The resulting $\Lambda(\bar{\Lambda})$ samples are about ten times larger than those obtained when using DIS cuts. In total, $N(\Lambda \to p\pi^-) = 1208413 \pm 1312$ and $N(\bar{\Lambda} \to p\pi^+) = 654387 \pm 1067$ events were reconstructed. The Σ^* hyperon signals are also enhanced. The number of Σ^* resulting from the fits are: $N(\Sigma^{*+}) = 44780 \pm 1301$, $N(\Sigma^{*-}) = 22716 \pm 872$, $N(\bar{\Sigma}^{*-}) = 37728 \pm 1361$ and $N(\bar{\Sigma}^{*+}) = 19813 \pm 1169$.

[3] The quoted numbers of NOMAD are not corrected for acceptance. Nevertheless, as shown in Ref. [4], the acceptance uncorrected ratios Σ^{*+}/Λ and Σ^{*-}/Λ in the full x_F region are practically the same as the corrected ones. As a good approximation one may expect the same behavior for the current fragmentation region.

The numbers of Ξ hyperons are: $N(\Xi^-) = 20458 \pm 162$ and $N(\bar{\Xi}^+) = 11448 \pm 128$. The invariant mass distributions for Λ, Σ^{*+}, Σ^{*-}, Ξ^- and their antiparticles without DIS cuts are given in the Appendix. In Table 2 the relative heavy hyperons yield ratios obtained using DIS and non-DIS $\Lambda(\bar{\Lambda})$ samples are given. One can see that within the experimental uncertainties the yield ratios for both samples are compartible.

The average Q^2 for this sample drops to $\langle Q^2 \rangle = 0.47$ (GeV/c)^2, as compared to $\langle Q^2 \rangle = 3.58$ (GeV/c)^2 when using the DIS cut. This observation indicates that the measured yield ratios are not strongly depending on Q^2. A check of the y dependence of the results was also made. The y interval was divided in 2 bins, larger and smaller than $y = 0.5$. The ratios were calculated in these bins with and without Q^2 cut. In each y bin the ratios with and without Q^2 cut are compatible within statistical uncertainties. The ratios in the large-y bin show a tendency to be on average $\sim$15 % higher than those in the small-y bin.

The ratios of production yields between heavy hyperons and Λ particles are important for the interpretation of the results on the longitudinal polarisation transfer in DIS. Indeed, a Λ hyperon originating from the decay of a heavier hyperon is polarised differently than the directly produced Λ particle. The indirectly produced Λ mainly come from the decay of Σ^0, Σ^{*+}, and Ξ hyperons. In Ref. [1], the contribution of the indirectly produced Λ was estimated by a Monte Carlo simulation to be as large as 60 %. Our Monte Carlo simulation with LEPTO default parameters shows that this contribution is about 58 % for Λ and 54 % for $\bar{\Lambda}$. With tuned LEPTO parameters (discussed further below) the fractions of the indirectly produced Λ and $\bar{\Lambda}$ are reduced to 37 % and 32 %, respectively.

Only the contributions from charged heavy hyperons were considered in the present analysis. The contribution from radiative decay $\Sigma^0 \to \Lambda + \gamma$ can only be indirectly

Table 2 Heavy hyperon to Λ and antihyperon to $\bar{\Lambda}$ yield ratios without DIS cuts normalized to the same ratios with DIS cuts

	Relative yield ratios without/with DIS cuts
Σ^{*+}/Λ	1.03 ± 0.08(stat)
$\bar{\Sigma}^{*-}/\bar{\Lambda}$	0.97 ± 0.11(stat)
Σ^{*-}/Λ	1.03 ± 0.16(stat)
$\bar{\Sigma}^{*+}/\bar{\Lambda}$	0.97 ± 0.13(stat)
Ξ^-/Λ	1.06 ± 0.09(stat)
$\bar{\Xi}^+/\bar{\Lambda}$	1.06 ± 0.09(stat)

Table 3 The heavy hyperon to Λ yield ratios in DIS

Ratios	LEPTO (Default)	COMPASS data	LEPTO (COMPASS)
$\Lambda/\bar{\Lambda}$	1.22 ± 0.01	1.71 ± 0.02	1.72 ± 0.01
K^0/Λ	6.06 ± 0.01	6.21 ± 0.05	6.22 ± 0.01
Σ^{*+}/Λ	0.082 ± 0.001	0.055 ± 0.005	0.052 ± 0.001
$\bar{\Sigma}^{*-}/\bar{\Lambda}$	0.074 ± 0.001	0.047 ± 0.006	0.038 ± 0.001
Σ^{*-}/Λ	0.084 ± 0.001	0.056 ± 0.009	0.067 ± 0.001
$\bar{\Sigma}^{*+}/\bar{\Lambda}$	0.060 ± 0.001	0.039 ± 0.006	0.037 ± 0.001
Ξ^-/Λ	0.051 ± 0.001	0.038 ± 0.003	0.029 ± 0.001
$\bar{\Xi}^+/\bar{\Lambda}$	0.056 ± 0.001	0.043 ± 0.004	0.040 ± 0.001
Σ^0/Λ	0.200 ± 0.003	–	0.130 ± 0.002
$\bar{\Sigma}^0/\bar{\Lambda}$	0.200 ± 0.003	–	0.120 ± 0.002

Table 4 The default and COMPASS-tuned LEPTO/JETSET parameters

Parameters	Default	COMPASS
PARJ(1)	0.1	0.03
PARJ(2)	0.3	0.45
PARJ(3)	0.4	0.175
PARJ(4)	0.05	0.078
PARJ(5)	0.5	3.0
PARJ(7)	0.5	0.13

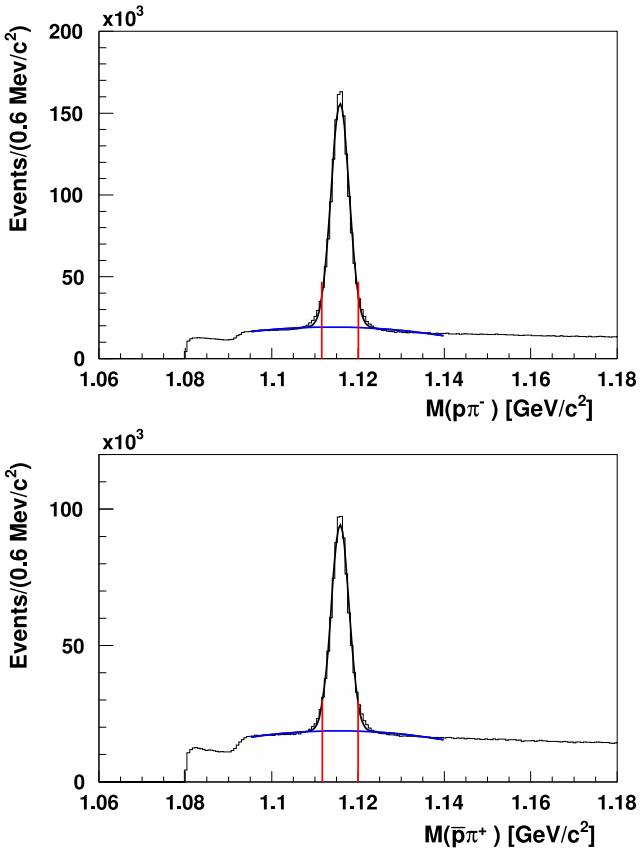

Fig. 5 The $p\pi^-$ (*top*) and $\bar{p}\pi^+$ (*bottom*) invariant mass distributions without DIS cuts. The total numbers of Λ and $\bar{\Lambda}$ determined within the fit interval are $N(\Lambda) = 1208413 \pm 1312$ and $N(\bar{\Lambda}) = 654387 \pm 1067$

estimated using the LEPTO simulation code, in which the final-state hadronisation is described by the Lund string fragmentation model. The production yield ratios calculated with the LEPTO default parameters are given in the first column of Table 3. Their comparison with the COMPASS results given in the second column shows that this simulation overestimates the experimental ratios for heavy hyperons by about ∼1.5. The Λ to $\bar{\Lambda}$ ratio exhibits an opposite trend whereas the K^0/Λ ratio is close to the experimental value.

In order to reproduce better the measured ratios given in Table 3, the LEPTO/ JETSET 7.4 parameters [12] related to the production yields of strange baryons were tuned (see Table 4). These parameters characterize the properties of the LEPTO generator not associated with kinematic distributions of hyperons: PARJ(1)—suppression of diquark-

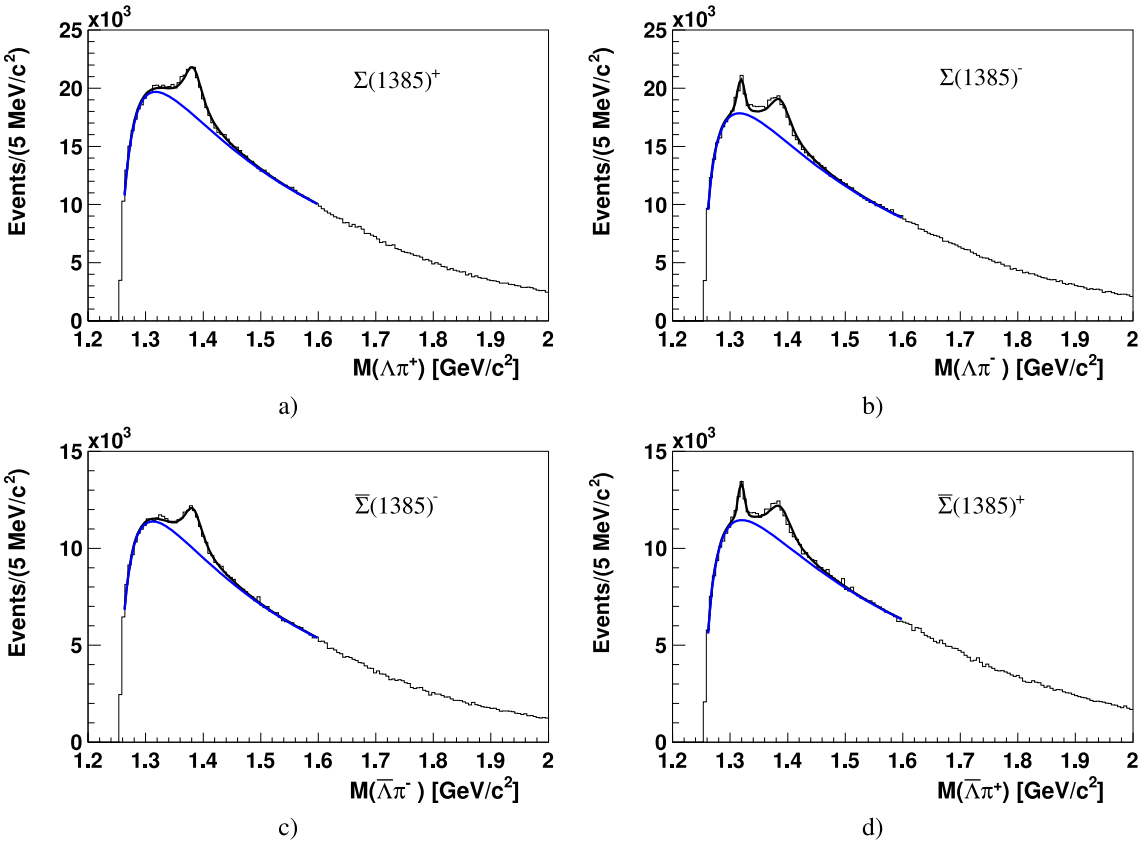

Fig. 6 The $\Lambda\pi$ invariant mass distributions without DIS cuts. The *solid lines* represent the signal plus backgroud and the background only obtained from the fit. The number of Σ^* resulting from the fits are: (**a**) $N(\Sigma^{*+}) = 44780 \pm 1301$, (**b**) $N(\Sigma^{*-}) = 22716 \pm 872$, (**c**) $N(\bar{\Sigma}^{*-}) = 37728 \pm 1361$ and (**d**) $N(\bar{\Sigma}^{*+}) = 19813 \pm 1169$

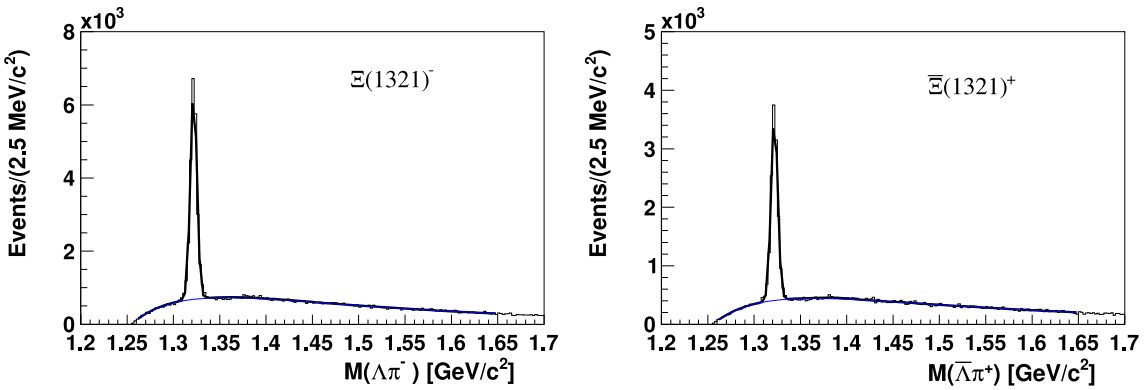

Fig. 7 Invariant mass distributions for $\Lambda\pi^-$ (*left*) and $\bar{\Lambda}\pi^+$ (*right*) pairs without the DIS cuts. The *solid lines* represent the signal plus backgroud and the background only obtained from the fit. The estimated numbers of Ξ hyperons are: $N(\Xi^-) = 20458 \pm 162$ and $N(\bar{\Xi}^+) = 11448 \pm 128$

antidiquark pair production in the colour field; PARJ(2)—suppression of $s\bar{s}$-pair production compared to $u\bar{u}$- or $d\bar{d}$-pair production; PARJ(3)—extra suppression of strange diquark production compared to the normal suppression of strange quarks; PARJ(4)—suppression of spin-1 diquarks compared to spin-0 ones; PARJ(5)—relative occurrence of baryon-antibaryon production; PARJ(7)—strange meson suppression factor. A study of the MC distributions of the common SIDIS Q^2 and W and the baryon variables z and p_T for Λ, Σ^*, Ξ and their antiparticles was performed. The distributions of two MC data sets, with default and tuned parameters, were found to be consistent within errors. The Q^2, W, z and p_T ratios of real data and Monte Carlo samples with both tuned and default parameters are similar without strong deviations from unity.

The simulated results obtained with the tuned parameters are shown in the third column of Table 3. The measured ratios of the heavy hyperon to Λ yields are now well reproduced. In addition, the agreement between the data and LEPTO for the Λ to $\bar{\Lambda}$, and K to Λ ratios is now very good. Finally, the new parameters also modify the unmeasured Σ^0/Λ ratio.

For completeness, the acceptance corrections were recalculated using the newly tuned LEPTO parameters. The new and old corrections agree within one standard deviation. The difference was included in the systematic uncertainties, mentioned at the beginning of this section.

6 Conclusions

The heavy hyperon to Λ and heavy antihyperon to $\bar{\Lambda}$ yield ratios were measured for the first time in charged lepton deep-inelastic scattering. All yield ratios were found to be in the range 3.8 % to 5.6 %. Within the relative uncertainties of about 10 %, the yield ratios for hyperons and antihyperons are quite similar. No strong Q^2 dependence of the ratios was found within the statistical accuracy. The obtained results imply that some parameters of the LEPTO code, which are associated with strange quark production and fragmentation in charged lepton DIS processes, should be substantially modified. Using the tuned LEPTO parameters, the fractions of indirectly produced Λ and $\bar{\Lambda}$ hyperons were found to be 37 % and 32 %, respectively.

Acknowledgements We gratefully acknowledge the support of the CERN management and staff, the skill and effort of the technicians of our collaborating institutes. Special thanks are due to V. Anosov and V. Pesaro for their technical support during installation and running of this experiment. It is a pleasure to thank S. Belostotsky, D. Naumov and Yu. Naryshkin for stimulating discussions.

Appendix: The sample without DIS cuts

The cuts on the four-momentum squared of the virtual photon, $Q^2 > 1$ (GeV/c)^2, and on the fractional energy y of the virtual photon, $0.2 < y < 0.9$ were ommited here but all other cuts were kept as in the DIS sample. The invariant mass distributions for Λ, Σ^{*+}, Σ^{*-},Ξ^- and their antiparticles are shown in Figs. 5, 6, 7.

References

1. A. Airapetian et al. (HERMES Collaboration), Phys. Rev. D **74**, 072004 (2006)
2. M. Alekseev et al. (COMPASS Collaboration), Eur. J. Phys. **64**, 171 (2009)
3. A.E.G. Ingelman, A. Edin, J. Rathsman, Comput. Phys. Commun. **101**, 108 (1997)
4. P. Astier et al. (NOMAD Collaboration), Nucl. Phys. B **621**, 3 (2002)
5. P. Abbon et al. (COMPASS Collaboration), Nucl. Instrum. Methods A **577**, 455 (2007)
6. P. Astier et al. (NOMAD Collaboration), Nucl. Phys. B **588**, 3 (2000)
7. P. Astier et al. (NOMAD Collaboration), Nucl. Phys. B **605**, 3 (2001)
8. M.R. Adams et al. (E665 Collaboration), Eur. Phys. J. C **17**, 263 (2000)
9. Q. Xu (STAR Collaboration), in *Proc. 17th International Spin Physics Symposium (SPIN06)*, Kyoto. AIP Conference Proceedings, vol. 915 (2006), p. 428. hep-ex/0612035
10. Review of Particle Properties. J. Phys. G **37**, 7A 075021 (2010)
11. E.S. Ageev et al. (COMPASS Collaboration), Eur. Phys. J. C **41**, 469 (2005)
12. T. Sjöstrand, Comput. Phys. Commun. **82**, 74 (1994)